ACS SENSORS

Perspective

Cite This: ACS Sens. 2019, 4, 782−791

pubs.acs.org/acssensors

Noble Metal Nanoparticle-Based Multicolor Immunoassays: An Approach toward Visual Quantification of the Analytes with the Naked Eye

Xiaoming Ma,[†,‡] Shan He,[†] Bin Qiu,[‡] Fang Luo,[§] Longhua Guo,*[,‡] and Zhenyu Lin*[,‡]

[†]School of Chemistry and Chemical Engineering, Key Laboratory of Organo-pharmaceutical Chemistry of Jiangxi Province, Gannan Normal University, Ganzhou, 341000, China

[‡]Institute of Nanomedicine and Nanobiosensing, Ministry of Education Key Laboratory of Analysis and Detection Technology for Food Safety (Fuzhou University), School of Chemistry and [§]College of Biological Science and Technology, Fuzhou University, Fuzhou, 350116, China

ABSTRACT: Noble metal nanoparticle-based colorimetric sensors have become powerful tools for the detection of different targets with convenient readout. Among the many types of nanomaterials, noble metal nanoparticles exhibit extraordinary optical responses mainly due to their excellent localized surface plasmon resonance (LSPR) properties. The absorption spectrum of the noble metal nanoparticles was mostly in the visible range. This property enables the visual detection of various analytes with the naked eye. Among numerous color change modes, the way that different concentrations of targets represent vivid color changes has been brought to the forefront because the color distinction capability of normal human eyes is usually better than the intensity change capability. We review the state of the art in noble metal nanoparticle-based multicolor colorimetric strategies adopted for visual quantification by the naked eye. These multicolor strategies based on different means of morphology transformation are classified into two categories, namely, the etching of nanoparticles and the growth of nanoparticles. We highlight recent progress on the different means by which biocatalytic reactions mediated LSPR modulation signal generation and their applications in the construction of multicolor immunoassays. We also discuss the current challenges associated with multicolor colorimetric sensors during actual sample detection and propose the future development of next-generation multicolor qualification strategies.

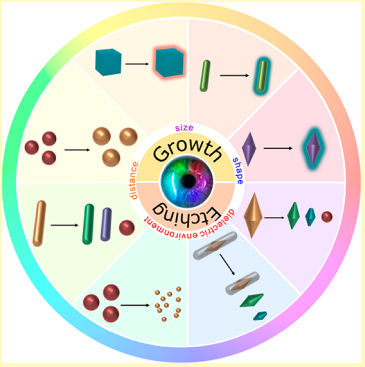

KEYWORDS: *multicolor immunoassays, localized surface plasmon resonance, colorimetric sensor, noble metal nanoparticles, biosensor, etching, growth*

With the merits of cost-effectiveness, simplicity of detection, and direct readout, colorimetric methods are widely used as a robust tool for detection of a variety of analytes.[1−3] Conventional colorimetric methods are mainly based on the interaction between organic dye probes and targets.[4,5] The transformation of chromogenic substance with the color change from colorless to a vivid color display can be observed with the naked eye or qualified by a simple UV−vis spectrum.[6,7] However, most of the traditional dye-based colorimetric assays are normally low sensitivity and limited by available analytes because most of the organic dyes exhibit low extinction coefficients.

In comparison, noble metal nanoparticles exhibit much higher extinction coefficients, especially gold and silver nanomaterials, 1000 times higher than that of organic dyes in the visible region, resulting in a nanomolar level (even lower range) sensitivity with a tunable dynamic range.[8,9] These excellent optical properties are due to their unique localized surface plasmon resonance (LSPR), which is caused by free electron oscillation on the metal surface under light stimulation.[10] The intensity and frequency of the LSPR band are highly confined to the size, shape, composition, dielectric environment, and distance of the colloidal nanoparticles or other nanostructures.[11] Therefore, the LSPR-based plasmonic colorimetric sensors have been applied to construct colorimetric sensing platforms for various targets, including biomarkers, bacteria, organic contaminants, DNA, and small molecules.[12−17]

Over the past decades, noble metal nanoparticles have been widely used for the fabrication of diverse colorimetric sensors. As shown in Figure 1, these sensing strategies can be divided into two categories: (a) monochrome change, such as mimic enzyme catalysis and aggregation of nanoparticles;[18−20] and (b) multicolor change, such as etching and growth of nanoparticles.[21,22] The monochrome colorimetric sensing platforms based on the aggregation mechanism mostly employed noble metal nanoparticles as the sensing unit, such as gold nanoparticles (AuNPs) and silver nanoparticles (AgNPs).[23−29] Typically, the color generation is caused by a

Received: March 3, 2019
Accepted: March 21, 2019
Published: March 21, 2019

DOI: 10.1021/acssensors.9b00438
ACS Sens. 2019, 4, 782−791

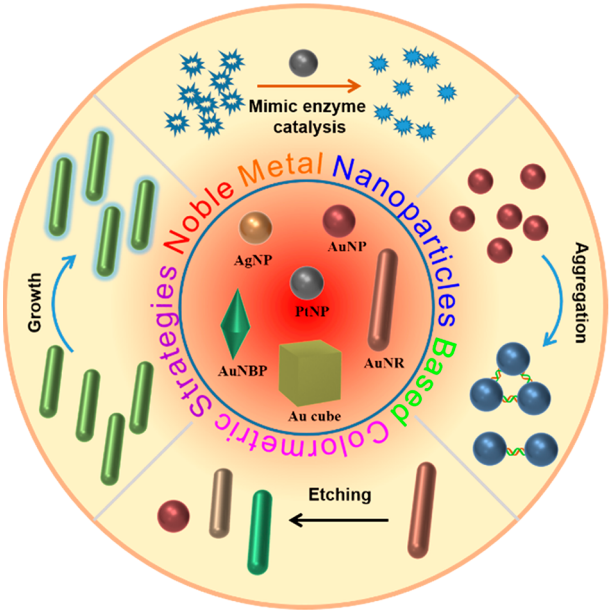

Figure 1. Scheme of noble metal nanoparticle based colorimetric strategies.

strong plasmon coupling between the nearby particles. The morphology, size, or distance variation of these nanoparticles leads to the plasmon band shift and an obvious color change.[30,31] The conventional LSPR-based plasmonic colorimetric platform usually exhibits high sensitivity and simple design, thereby enabling the ultrasensitive detection of target molecules. Although the conventional colorimetric platforms own relatively high sensitivity and versatility, the aggregation model of this colorimetric platform still faces several problems. First, external environment variation, such as temperature, pH, salt, and charged molecules, may also cause the nanoparticle aggregation.[32] This nonresponse aggregation would lead to false positive/negative results. Second, tedious modification of recognized molecules on the nanoparticles required sophisticated personnel and time-consuming preparation. Third, the intensity or limited kinds of color change of the solution are unsuitable for determination by the naked eye, since human eyes are sensitive to the kinds of color change compared to the intensity variation, resulting in difficulty of colorimetric qualification with the naked eye.

Over the past few decades, the plasmonic sensor with multicolor change has become a newly developing research field. The main factor for successful polychromatic change is that in which the LSPR variation of nanoparticles covers most of the visible absorption spectrum. The LSPR is sensitive to the variation of size, shape, and dielectric environment of the nanoparticles, and thereby the etching or growth of nanoparticles leading to the change of plasmon band. The multicolor plasmonic sensors show significant optical property improvement toward monochromic biosensors, such as the following: (1) most of these nanoparticles constructed for multicolor sensing were stable in the complex matrix; (2) the color change of the multicolor platform was more abundant than that of the conventional single color change; (3) the majority of multicolor biosensors were conducted directly with any complicated modification. Therefore, growing research attention was focused on the construction of multicolor sensors for different analytes.

Although numerous excellent plasmonic colorimetric platforms have been extensively reviewed, most of them are focused on the aggregation modules, while the multicolor colorimetric platforms have rarely been reported.[33] Anisotropic nanoparticles have become a potential chromogenic substrate in multicolor sensing platforms due to their extraordinary optical property. For example, gold nanorods (AuNRs) possess two different plasmonic bands: one is the transverse mode band and the other corresponds to the longitudinal mode band.[34,35] The aspect ratio (length/width) is extremely sensitive to the size or morphology change.[36] The longitudinal band will shift with the variation of aspect ratio, causing a series of vivid color change as colorful as a rainbow.[37] Herein, we exclusively review the progress of multicolor immunoassays based on noblemetal nanoparticles and address their challenges and future directions in the construction of colorimetric sensors.

GENERAL MECHANISMS AND DIFFERENT STRATEGIES FOR MULTICOLOR IMMUNOASSAYS

A variety of colors have significantly improved the accuracy of colorimetric detection with the naked eye. To ensure that this colorimetric strategy can be easily carried out, a colorimetric standard card corresponding to the standard concentration of target must be constructed. Typically, the multicolor standard card was similar to pH test strips, whereas the concentration of H^+ can be quickly read out by the color distinction. Therefore, a suitable multicolor substrate must be selected which is essential for vivid color display. Second, the relationship between target concentration and color change should be constructed. Specifically, different concentrations of standard solutions were tested, and the color display according to a certain concentration of target was recorded. Typically, the procedure for visual quantification of an unknown concentration of sample was as follows: (1) compare the color of unknown sample according to the established multicolor standard card; (2) select a proper standard reference with nearly the same color change; (3) in case the color of the sample was in between the colors of two neighboring standard solutions, the average concentration of these two standard solutions was designated as the sample concentration.[38]

Noble Metal Nanoparticle-Etching-Based Multicolor Immunoassays. The enzyme is a natural catalyst which can extensively improve the capability for substance decomposition, leading to significant signal amplification. Meanwhile, the robust strategies of enzyme-labeling on the antibody or DNA can dramatically improve the possibility for sensitive detection of DNA, RNA, protein, and small molecules.[39−43] In conventional ELISA assays, horseradish peroxide (HRP) is an important heme-containing enzyme which can biocatalyze the oxidation of enzyme-specific chromogenic substrates (e.g., 3,3′,5,5′-tetramethylbenzidine (TMB) and 2,2′-azino-bis(3-ethylbenzothiazoline-6-sulfonic acid) (ABTS)) from colorless into colored products, and the intensity signal of the solution can be analyzed by a microplate reader or the naked eye.[44−48] Although the conventional antibody−antigen immunoassays have been successfully transferred into colorimetric readout, the monochromic color changes have drastically curtailed the sensitivity and selectivity of visual detection with the naked eye.[49,50] Therefore, a vast amount of color change caused by the different concentrations of analytes is of paramount importance and can obviously improve the accuracy of detection.

DOI: 10.1021/acssensors.9b00438
ACS Sens. 2019, 4, 782−791

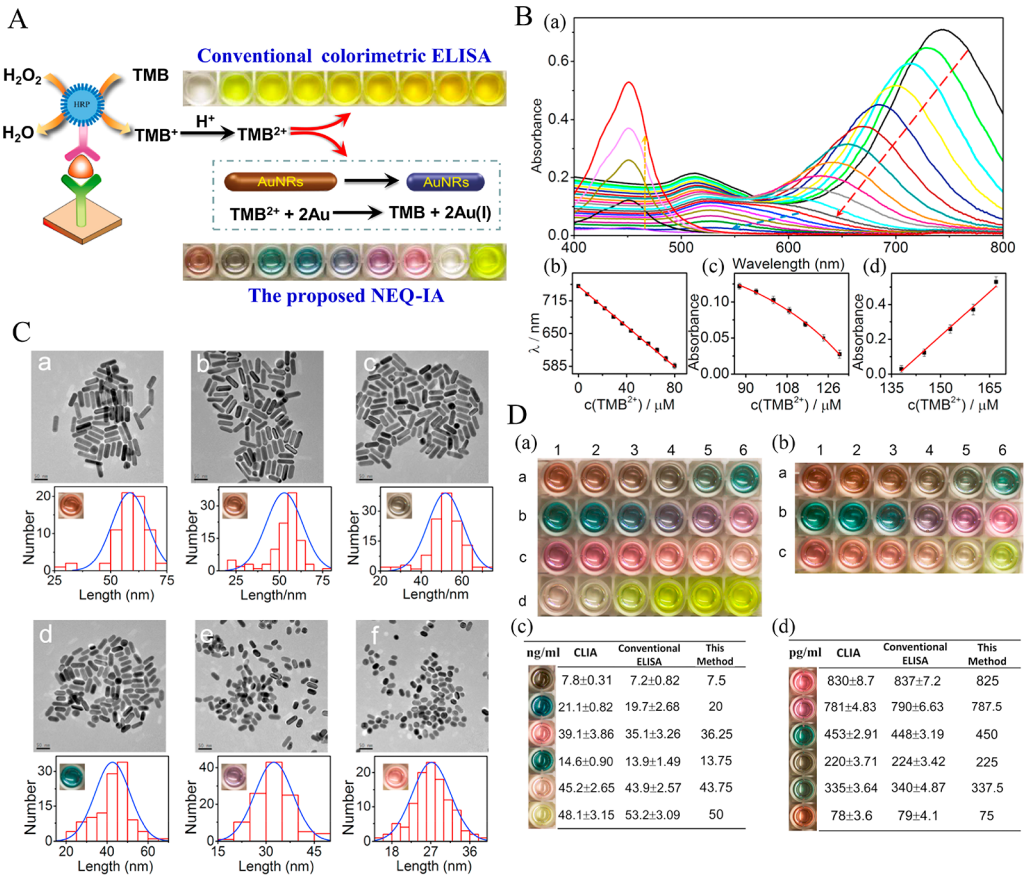

Figure 2. (A) Schematic illustration of multicolor immunosensor for visualization detection based on TMB^{2+} mediated etching of AuNRs. (B) UV spectra of the solution after the reaction between AuNRs with different concentrations of TMB^{2+} (a-d). (C) Corresponding TEM images, statistical analysis, and solution color of the AuNRs after reaction with TMB^{2+} (a-f). (D) Colorimetric plasmonic ELISA detection of CEA (a) and PSA (b); the comparison of quantification results of CEA (c) and PSA (d) in the serum samples with different strategies. Reprinted with permission from ref 53. Copyright 2017 Elsevier.

TMB is a commonly used commercialized substrate for colorimetric assays.[51] Typically, the colorless TMB was oxidized into blue color (TMB^+) under the catalysis of HRP, and changed further into yellow (TMB^{2+}) in the acidic environment. Thus, analyte concentration can be measured by the absorbance of the colored solution.[52] Interestingly, the protonated TMB (TMB^{2+}) was found to be capable of etching AuNRs. We assume that the redox reaction can take place between AuNRs and TMB^{2+} because the standard electrode potential (E^{Θ}) of TMB^{2+}/TMB (0.741 V vs NHE) is higher than that of $AuBr^{2-}$−$(CTA)^{2+}$/Au in the presence of CTAB. For example, our group demonstrated that TMB^{2+} exhibits remarkable oxidative ability, and can act as an effective oxidation reagent to react with AuNRs at a certain stoichiometric ratio. The length of AuNRs was quantitatively etched and the solution color displays vast vivid changes (from brown to red as colorful as a rainbow) (Figure 2).[53] The detection procedure was carried out on an antibody−antigen sandwich structure. This multicolor display was conducted on the conventional HRP−TMB/H_2O_2 colorimetric system directly without any complex steps. The dominant factor of the solution color change is due to the fast etching of AuNRs (~90 s) without any colorimetric interference, thus allowing the rapid colorimetric detection of target molecules. The degree of blue-shift of AuNRs' longitudinal LSPR peak was linear to the increasing amount of target molecules added. Meanwhile, the numerous resulting color changes can easily be observed with the naked eye, thus allowing the semi-quantitative detection by visualization. This platform has been successfully applied for the detection of carcinoembryonic antigen (CEA) in human serum with a visual detection limit as low as 2.5 ng/mL. Furthermore, this strategy also applied to the prostate-specific antigen (PSA) detection with satisfactory results.

Because TMB/H_2O_2 is a versatile chromogenic substrate in the immunoassay system, our group also developed a multicolor glucose sensor for the rapid detection of glucose molecules in human urine samples with satisfactory results (Figure 3).[54] Herein, glucose oxidase (GOx) catalytically decomposed substrates (glucose and dissolved oxygen) into gluconic acid and H_2O_2. The resulting H_2O_2 molecules can also react with TMB by the catalysis of HRP, resulting in a wonderful colorful change when the AuNRs were added. Combined with this dual-enzyme catalysis system, the colorless glucose solution has sufficiently transferred into the multicolor display.

Furthermore, our group has also combined the TMB^{2+} mediated AuNRs etching strategy with enzyme inhibition of H_2S; the concentration of H_2S in the rat brain has been sufficiently detected coupled with microdialysate (Figure 4).[55]

DOI: 10.1021/acssensors.9b00438
ACS Sens. 2019, 4, 782−791

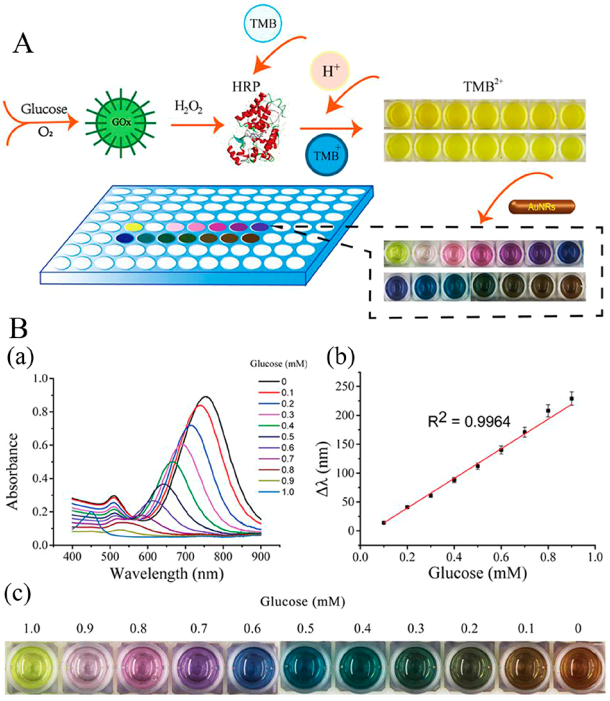

Figure 3. (A) Schematic illustration of multicolor colorimetric sensor for glucose detection. (B) UV−vis spectra of the AuNRs change (a); and the LSPR shift upon the addition of a different amount of glucose (b); visual inspection of glucose using the proposed plasmonic sensor (c). Reprinted with permission from ref 54. Copyright 2016 The Nature Publishing Group.

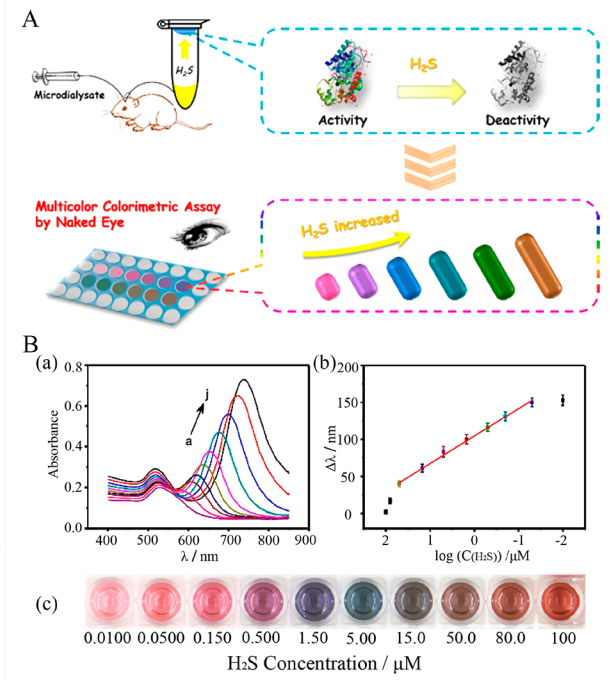

Figure 4. (A) Scheme illustration of multicolor colorimetric sensing platform for the detection of H_2S in the rat brain. The HRP was deactivated by H_2S, which then affects the etching degree of AuNRs with different amounts of TMB^{2+}, which results in vivid color change. (B) UV−vis spectra change (a); LSPR shift (b); and the corresponding color change of the solution as a function of H_2S (c). Reprinted with permission from ref 55. Copyright 2018 American Chemical Society.

It is of great significance to detect H_2S in the brain because the concentration of H_2S is a vital indicator of nerve disease, diabetes, and liver cirrhosis. It was found that H_2S can destroy the catalytic capability of HRP, and thus affected the amount of TMB^{2+} generated. Therefore, the relationship between the concentration of H_2S and solution color change was established according to the previously reported TMB^{2+} mediated oxidation of AuNRs. The concentration of H_2S can be successfully detected with the color change of the solution. This multicolor H_2S sensor has the advantages of simplicity, cost-effectiveness, and direct qualification without the assistance of any sophisticated types of equipment.

Specifically, previous studies have shown that hydrogen peroxide can effectively etching AuNRs at room temperature. However, the reaction rate is extremely low and requires a high concentration of H_2O_2.[56] In contrast, as for the Fenton's reaction which disproportionately breaks down H_2O_2 with the Fe^{2+} catalyst to produce hydroxyl radical (•OH), much stronger oxidation capability is shown over that of H_2O_2.[57] Therefore, based on this mechanism, H_2O_2−Fe^{2+} mediated etching of AuNRs was combined for the construction of a robust plasmonic colorimetric platform (Figure 5).[38] The concentration of H_2O_2 could be quantitatively controlled by the catalysis of catalase, thus regulating the etching degree of AuNRs at the same time. In this strategy, catalase serves as a powerful enzyme marker labeled with the detection antibody or DNA. The specific amount of H_2O_2 was quantitatively regulated by the as-formed enzyme tagged structure. Thus, upon the introduction of wanted targets, the aspect ratio of the AuNRs was dramatically decreased, accompanied by the extinction spectrum change, thereby inducing a vivid multicolor change of the solution. Therefore, this high-performance analytical strategy has formed the basis of visualization detection of DNA, RNA, proteins, and small molecules with a color change.

To measure the fish freshness, the concentration of hypoxanthine (Hx) is chosen as a fatal index during the detection.[58] Therefore, there is a great demand to develop a powerful, rapid, simple detection procedure of Hx. Due to the catalysis property of xanthine oxidase (XOD), H_2O_2 was generated quantitatively by the decomposition of Hx in the presence of dissolved O_2.[59−61] In this respect, XOD was utilized in enzyme-mediated AuNRs oxidation to evaluate the fish freshness with color distinction by the naked eye (Figure 6).[62] In this assay, the generated H_2O_2, which was produced by the catalytic decomposition of Hx, can transform to •OH with more effective oxidation capability upon the addition of Fe^{2+}. By virtue of its portability and easy visualization, the multicolor naked-eye fish freshness assessment has been successfully constructed and shown great potential application for in-field evaluation.

AuNanobipyramid@Ag Nanorods (AuNBP@Ag) show an extraordinary optical property similar to AuNRs. The extinction spectra of AuNBP@Ag can be modulated over the entire visible absorption spectrum, confirming the construction of multicolor immunosensors (Figure 7).[63] This detection is combined with the conventional sandwich immunoassay system whereas catalase was labeled on the detection antibody. The AuNBP@Ag was etched by the oxidation of •OH with the presence of target molecules. Compared to the conventional one-direction shifts of LSPR peak, AuNBP@Ag Nanorods exhibit the unusual peak movement. Specifically, the longitudinal LSPR peak of the solution blue-shifted first, and

DOI: 10.1021/acssensors.9b00438
ACS Sens. 2019, 4, 782−791

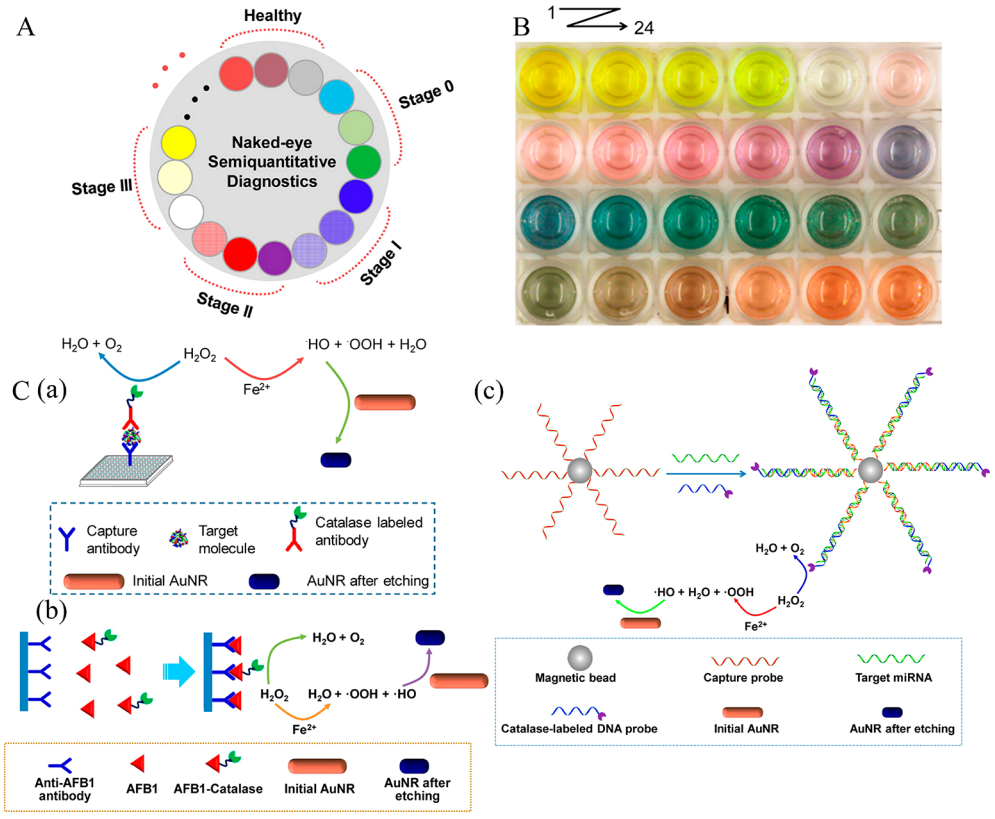

Figure 5. (A) Schematic illustration of the Fenton reaction-based multicolor colorimetric sensors. (B) Visual detection of different concentrations of α-fetoprotein (AFP) (0−120 ng/mL). (C) Schematic illustration of the multicolor colorimetric sensors for protein detection (a), aflatoxin B1 (AFB1) detection (b), and miRNA detection (c). Reprinted with permission from ref 38. Copyright 2016 American Chemical Society.

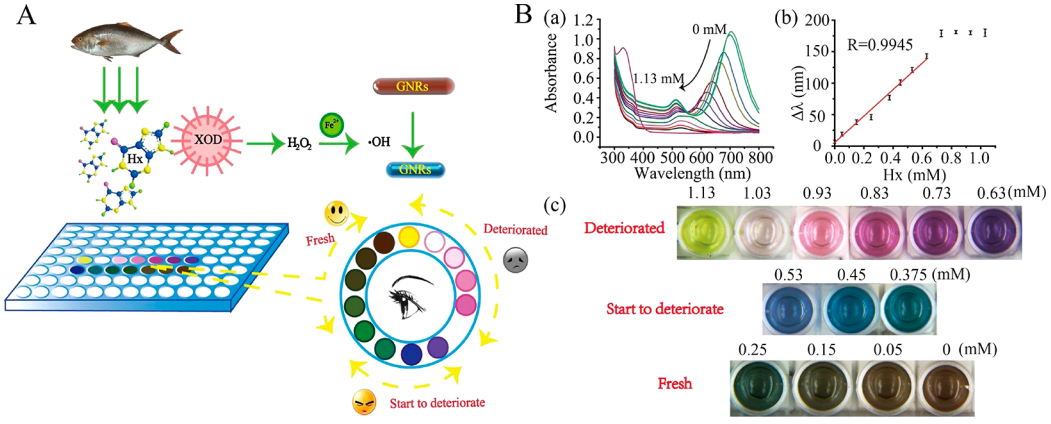

Figure 6. (A) Schematic illustration of the plasmonic multicolor colorimetric sensor for fish freshness measurement with the naked eye. (B) UV−vis spectra change of AuNRs (a); and the LSPR shift of AuNRs (b) in the presence of different concentration of Hx; the relationship between different kinds of color change and the concentrations of Hx variation (c). Reprinted with permission from ref 62. Copyright 2017 Elsevier.

then red-shifted, and then blue-shifted again. The resulting color of the solution shows similar interesting variations which are also related to different concentrations of squamous cell carcinoma antigen (SCCA). To improve the accuracy and sensitivity of the AuNBP@Ag-etching based colorimetric platform, the spectrum intensity and the peak position change of the AuNBP@Ag were combined for quantification. The colorimetric results showed a linear correlation in the concentration of SCCA from 2.5 to 105 ng/mL with a limit of detection of 0.85 ng/mL.

Ag nanoprisms also exhibit excellent optical properties, which were suitable for multicolor sensing. A convenient and sensitive colorimetric method using a homogeneous system (unmodified Ag nanoprisms and GOx contained) for the effective detection of glucose in serum was conducted.[64] The Ag triangular nanoprisms can be etched from triangular to round by H_2O_2 due to the enzymatic catalysis of glucose. Thus, the blue shift in LSPR can be observed with a color change from blue to mauve, which enables the visual and quantified detection of glucose. The detection limit was 2.0×10^{-7} M with a detection range from 2.0×10^{-7} to 1.0×10^{-4} M. Another application of Ag nanoprisms was the visual detection for DNA.[65] On the basis of inherent sensitivity of plasmonic Ag nanoprisms, the enzyme-mediated etching of silver

DOI: 10.1021/acssensors.9b00438
ACS Sens. 2019, 4, 782−791

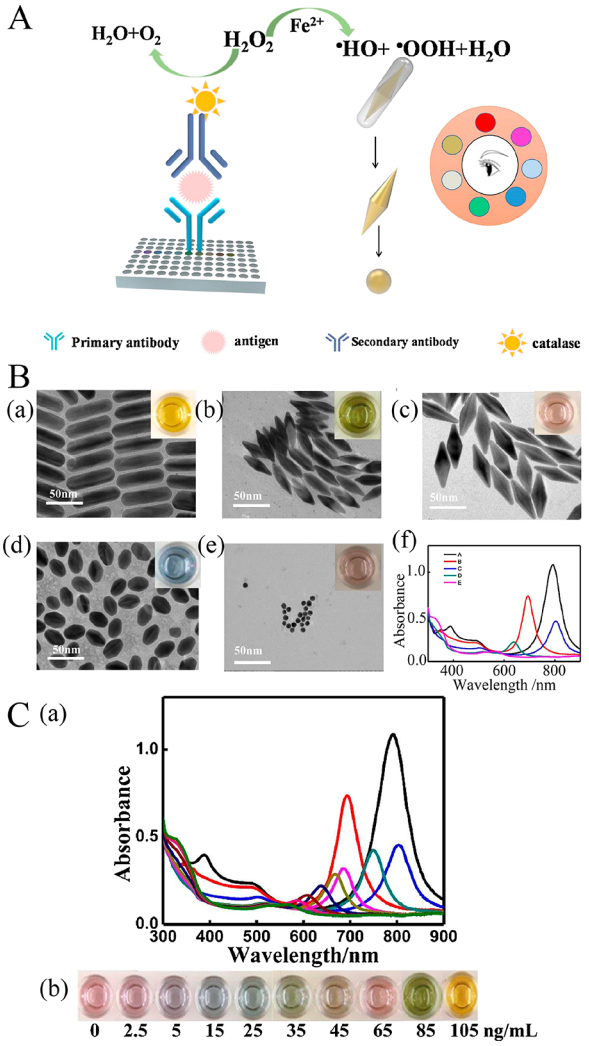

Figure 7. (A) Schematic illustration of multicolor colorimetric platform for the visualization detection of SCCA. Catalase labeled secondary antibody formed the sandwich structure and subsequently catalyzed the hydrolyzation of H_2O_2. The addition of Fe^{2+} catalyzes the remained H_2O_2 to generate •OH, consequently etching AuNBP@Ag to allow the colorimetric detection of SCCA. (B) Characterization of AuNBP@Ag reacts with different amount of H_2O_2. (C) UV−vis spectrum (a) and color imaging (b) results of the multicolor sensor for the detection of SCCA. Reprinted with permission from ref 63. Copyright 2018 Elsevier.

nanoprisms was applied for DNA deposition. In the presence of DNA, the silver nanoprisms were selectively oxidized by enzyme catalysis generated H_2O_2. The concentration of DNA can be detected by the color change with the naked eye or quantitatively with UV−vis equipment. Besides, silver nanoparticles or clusters with a specific shape show great potential for multicolor sensing.[66] The results demonstrated that a wide range of colors, sizes, and shapes can be selectively tuned by fine control of the reagent's molar concentrations.

Etching-based multicolor sensors can also be applied in the point-of-care-test (POCT) diagnosis. A multiplexed lateral flow POCT sensor was conducted for the detection of febrile illnesses based on the optical properties of Ag nanoparticles.[67] Different sizes of Ag nanoparticles were combined with three monoclonal antibodies through electrostatic adsorption mainly, which was favor to distinguish among different pathogens. Based on the merit of the multicolor change, the concentration of different biomarkers can be distinguished by the color of the test lines at the same time.

Nanoparticle Growth Based Multicolor Assays. As mentioned previously, the heteroepitaxial growth of nanoparticles leads to the form of a core−shell nanostructure. Variation of the size, shape, or composition in as-formed nanoparticles results in the LSPR spectral position change as well as solution color variation. Therefore, this mechanism paves a new avenue for the construction of plasmonic multicolor colorimetric sensors. In the conventional seed-mediated synthesis of AuNRs protocols, ascorbic acid (AA) is of vital importance because it not only acts as a reducing agent but also influences the morphology of materials. Alkaline phosphatase (ALP), a common commercially used enzyme in molecular diagnosis, was found to have the capability for catalytic hydrolysis of ascorbic acid 2-phosphate (AA-P) to generated AA.[68,69] Thus, ALP-mediated growth or etching of nanoparticles can be integrated with multicolor colorimetric platforms for the detection of various targets. Tang's group developed a multicolor colorimetric protocol for monitoring the activity of ALP based on the formation of gold/silver core/shell nanorod.[70] In this assay, the LSPR absorption of AuNRs was precisely tuned by enzyme-mediated deposition of silver nanoshell on the surface of gold AuNRs. Upon the addition of enzyme, the AA-P was hydrolyzed to generated the reductive ascorbic acid, which leads to the reduced silver coating on the AuNRs. Therefore, high-resolution color change due to the size variation of nanoparticles can effectively ensure visual detection by the naked eye. This proposed biosensor was much cheaper than the conventional colorimetric strategy, and the as-formed Au@Ag nanoshell can remain stable for a long time. Later on, Chen and co-workers reported a multicolor colorimetric platform of *Escherichia coli* detection in low-resource settings.[71] In this assay, the bacterial cells could be infected with T7 bacteriophages (phages), resulting in the release of *β*-gal for enzyme-induced colorimetric detection. In the presence of *β*-gal, *p*-aminophenol (PAP) was produced with the catalysis of the substrate *p*-aminophenyl *β*-D-galactopyranoside. Thereby, the enzyme-induced metallization led to the LSPR shifts and multicolor changes from light green to orange-red. In comparison to the conventional antibody-based platform, one of the most significant advantages is that the phage-based system not only shows excellent selectivity but also acts as a signal amplification strategy. This is advantageous compared to an antibody-based platform because of their specificity for target bacterial cells, their ability to distinguish between live and dead cells, and their low cost. Similarly, Gao's group demonstrated a highly efficient signal amplification assay for the sensitive detection of PSA with the naked eye.[72] On the basis of enzyme-catalyzed growth of the core/shell nanostructure, the silver shells were deposited on the AuNRs by the reduction of *p*-aminophenol, or dephosphorylation of *p*-aminophenol phosphate due to the catalysis of ALP. Consequently, in the presence of PSA, the LSPR plasmon band blue-shifted accompanied by a series of color changes. This assay was successfully applied for visualizing the detection of the PSA concentration with the naked eye, which was 10^4-fold higher than the conventional colorimetric ELISA assay.

As another example, our group revealed that AA-controlled in situ growth of gold nanoparticles was suitable for the multicolor ELISA platform construction.[73] The labeled ALP efficiently triggered the removal of the phosphate group from AA-P to produce AA, thus providing a basic reducing reagent

DOI: 10.1021/acssensors.9b00438
ACS Sens. 2019, 4, 782−791

for in situ growth of AuNRs. The as-generated different amounts of ascorbic acid added to the starting solution result in the formation of AuNRs with narrow size distributions and different aspect ratios. As a result, the ALP-mediated in situ growth of AuNRs displayed rich color change in response to the concentration of target molecule variation (Figure 8A). By

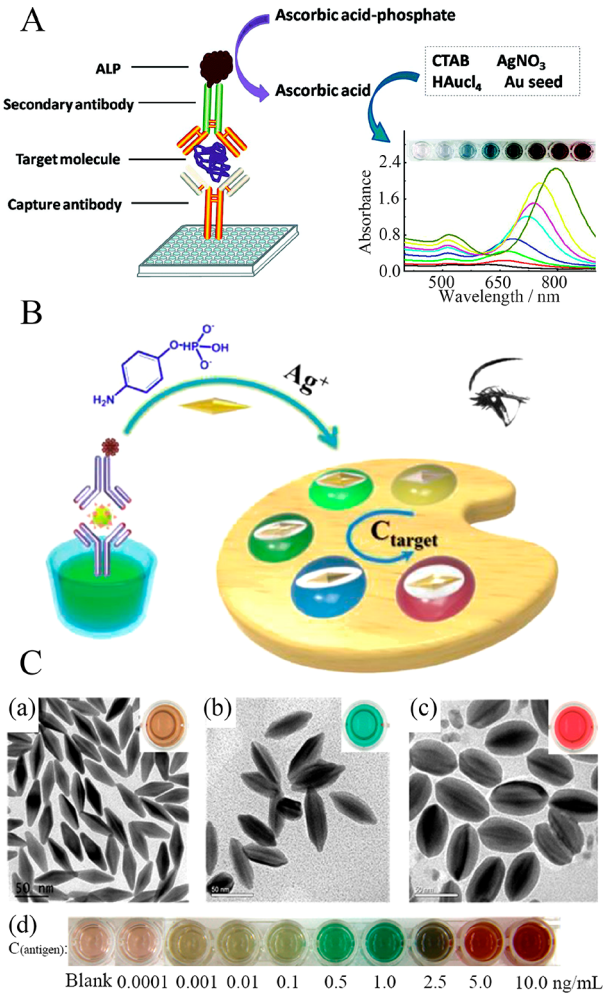

Figure 8. (A) Scheme of ALP-mediated in situ growth of AuNRs colorimetric biosensor. Reprinted with permission from ref 73. Copyright 2016 Royal Society of Chemistry. (B) Scheme of growth of AuNBPs based on the catalysis of ALP. (C) TEM (a-c) and color images (d) of AuNBPs in the presence of different concentration of H5N1. Reprinted with permission from ref 74. Copyright 2016 American Chemical Society.

virtue of this strategy, the proposed plasmonic multicolor sensors ensure detection of ultralow concentration of PSA by the naked eye with a detection limit as low as 1×10^{-15} g/mL. The linear dynamic range was from 10^{-3} to 200 pg/mL, indicating their potential applicability for the identification of ultralow concentration of disease biomarkers in a wide linear range with the naked eye.

It is reported that AuNBPs shows narrow plasmonic line widths with good stability. The deposition of the silver monomer on the surface of AuNBPs leads to the LSPR peak shift and multicolor change of the detection solution.[74] The 4-aminophenol, which was generated during the catalyzed dephosphorylation of *p*-aminophenol phosphate by ALP, can reduce the silver ions to generated a silver shell on the surface of AuNBPs. Upon the addition of target molecules, the longitudinal LSPR band of as-formed AuNBP@Ag starts to blue-shift, accompanied with vivid color variation. Notably, this technique is successfully applied to detect H5N1 virus with satisfactory results (Figure 8D). The LOD was as low as 1 pg/mL with a wide linear range from 0.001 to 2.5 ng/mL for the detection of H5N1 virus antigen. This growth of AuNBP platform shows much better sensitivity compared to the other nanoparticle growth strategies.

In addition, gold nanocages can also used for the construction of multicolor biosensor by the formation of gold/silver core/shell structure.[75] For example, Wang's group utilized gold nanocages for the sensitive colorimetric detection of AA.[76] Specifically, in the presence of AA, silver shells from the reduction of Ag^+ ions were grown on the surface of gold nanocages. Thereby, the Au@Ag nanocages was formed instead of self-nucleation. Because both the morphology and the component were transformed due to the silver deposition, the LSPR of as-formed Au@Ag nanocages shifts to a shorter wavelength with a perceptible color change. Here, the concentration of AA in the range from 0.05 to 7.5 μM was detected and the quantitative test results can be directly read out by the naked eye. In another example from Gao et al., they designed a plasmonic colorimetric strategy based on the enzyme guided silver deposition on gold nanostars (AuNS).[77] In this study, they found that the growth of Au@Ag nanostars results in a substantial blue-shift of the LSPR peak accompanied by different kinds of color change from blue to orange. To improve the detection sensitivity, they combined both the hybridization chain reaction signal amplification and the enzyme catalysis. Here, as a proof-of-concept, the Au@Ag nanostars was formed upon the addition of different concentrations of DNA. The concentration of DNA in the range of 10 fM to 50 pM was successfully detected, and this proposed strategy could be easily extended for the other applications due to the assistance of conventionally used ALP as a label.

CONCLUSIONS AND PERSPECTIVES

In this Perspective, the noble metal nanoparticle-based multicolor immunoassays have been elaborately discussed. We summarized the general mechanisms and discussed in detail different strategies for multicolor immunoassays. Compared to the conventional nanoparticle aggregation based colorimetric strategies, the growth or etching of nanoparticles based multicolor plasmonic sensors shows remarkable advantages in colorimetric immunoassays. First, the as-prepared nanoparticles can be used directly without further modification, thus remarkably improving the detection efficiency. Second, these detection platforms are stable due to the surfactant coated surface of nanoparticles; therefore, no false response would be yielded by the autoaggregation of nanoparticles and allow ultrasensitive determination under complex matrix. Third, the concentration of the solution can be directly read out by different kinds of color change with the naked eye, and the multicolor display has extensively improved the detection accuracy. Therefore, the applications of multicolor immunoassays are spread through various applications, including food safety analysis, environmental pollutant detection, and point-of-care testing.[78,79]

However, several critical issues still need to be addressed before the broader application of noble metal nanoparticle-based colorimetric sensors. Because the multicolor platforms

DOI: 10.1021/acssensors.9b00438
ACS Sens. 2019, 4, 782−791

are mainly established by the growth or etching mechanisms of nanoparticles, it is vitally important to obtain highly uniform materials with stable optical and chemical properties. However, current approaches for the preparation of nanoparticles could not afford the requirement of synthesizing highly uniform nanomaterials for wide-scale applications. Besides, most of the traditional synthetic protocols require long incubation time and tedious washing steps, which dramatically limited the practical applications of these sensors. Moreover, the relationship between solution color change and morphology, size, or composition of nanoparticles as yet lack theoretical calculation. Computer simulations will become a powerful tool for suitable nanomaterial candidate selection. An example application is analyzing the structure of the anisotropic nanoparticles (such as AuNRs, Au flowers, and Au@AgNRs), which is being studied using FDTD modeling in combination with scanning tunneling microscopy, low-energy electron diffraction, and surface-sensitive X-ray spectroscopic techniques. Therefore, many efforts should pay attention to producing a large number of stable nanomaterials in the future.

Motivated by the point-of-care testing diagnostic applications, the multicolor sensing will undergo further improvement to meet the requirement of practical applications. First, the enzyme catalyst-based growth or etching of nanoparticles has the common disadvantage of long-term catalytic reaction time. Second, the transformation in sizes, shapes, or morphologies of plasmonic nanoparticles is susceptible to the external complicated environment. Third, most of the multicolor colorimetric systems are constructed in the solution system, which is not convenient for further household use.

Quantitative detection of target molecules is critical for the construction of noble metal nanomaterial-based multicolor colorimetric platforms in practical applications. Although the abundant kinds of color change have met the needs of more accurate detection with the naked eye, the color discrimination with the naked eye could merely afford the semiqualifications. Thereby, the integration of multicolor display and smartphones or wearable devices could further expend the qualified application of plasmon-based colorimetric diagnostic.

In summary, a vast amount of excellent multicolor immunoassays show significant advantages compared to the traditional colorimetric assays that form a solid foundation for the in-field and point-of-care testing applications. The transformation of this technique from the laboratory to large-scale application brings both opportunity and challenge.

AUTHOR INFORMATION

Corresponding Authors

*(L.G.) E-mail: guolh@fzu.edu.cn.

*(Z.L.) E-mail: zylin@fzu.edu.cn.

ORCID

Longhua Guo: 0000-0003-0706-0973

Zhenyu Lin: 0000-0001-7890-6812

Notes

The authors declare no competing financial interest.

ACKNOWLEDGMENTS

This work was financially supported by the National Sciences Foundation of China (21575027, 21675028, and 21804022), the cooperative project of production and study in University of Fujian Province (2018Y4007), STS Key Project of Fujian Province (2017T3007), the Program for New Century Excellent Talents in Fujian Province University, the Program for Changjiang Scholars and Innovative Research Team in University (No. IRT15R11), and the Science and Technology Project of the Education Department of Jiangxi Province of China (No. GJJ170846).

ABBREVIATIONS

LSPR, localized surface plasmon resonance; AuNPs, gold nanoparticles; AgNPs, silver nanoparticles; AuNRs, gold nanorods; HRP, horseradish peroxide; TMB, 3,3′,5,5′-tetramethylbenzidine; ABTS, 2,2′-azino-bis(3-ethylbenzothiazoline-6-sulfonic acid); CEA, carcinoembryonic antigen; PSA, prostate-specific antigen; Gox, glucose oxidase; AFB1, aflatoxin B1; AFP, alpha-fetoprotein; Hx, hypoxanthine; XOD, xanthine oxidase; AuNBP@Ag, AuNanobipyramid@Ag Nanorods; SCCA, squamous cell carcinoma antigen; AA, ascorbic acid; ALP, alkaline phosphatase; AA-P, ascorbic acid 2-phosphate; ELISA, enzyme-linked immunosorbent assay; POCT, point-of-care-test; PAP, *p*-aminophenol; AuNS, gold nanostars

REFERENCES

(1) Howes, P. D.; Rana, S.; Stevens, M. M. Plasmonic nanomaterials for biodiagnostics. *Chem. Soc. Rev.* **2014**, *43* (11), 3835−3853.

(2) Kailasa, S. K.; Koduru, J. R.; Desai, M. L.; Park, T. J.; Singhal, R. K.; Basu, H. Recent progress on surface chemistry of plasmonic metal nanoparticles for colorimetric assay of drugs in pharmaceutical and biological samples. *TrAC, Trends Anal. Chem.* **2018**, *105*, 106−120.

(3) Zhou, D.; Xie, G.; Cao, X.; Chen, X.; Zhang, X.; Chen, H. Colorimetric determination of staphylococcal enterotoxin B via DNAzyme-guided growth of gold nanoparticles. *Microchim. Acta* **2016**, *183* (10), 2753−2760.

(4) Morsy, M. K.; Zor, K.; Kostesha, N.; Alstrøm, T. S.; Heiskanen, A.; El-Tanahi, H.; Sharoba, A.; Papkovsky, D.; Larsen, J.; Khalaf, H. Development and validation of a colorimetric sensor array for fish spoilage monitoring. *Food Control* **2016**, *60*, 346−352.

(5) Kumawat, L. K.; Mergu, N.; Asif, M.; Gupta, V. K. Novel synthesized antipyrine derivative based "Naked eye" colorimetric chemosensors for Al^{3+} and Cr^{3+}. *Sens. Actuators, B* **2016**, *231*, 847−859.

(6) Jin, L.; Meng, Z.; Zhang, Y.; Cai, S.; Zhang, Z.; Li, C.; Shang, L.; Shen, Y. Ultrasmall Pt nanoclusters as robust peroxidase mimics for colorimetric detection of glucose in human serum. *ACS Appl. Mater. Interfaces* **2017**, *9* (11), 10027−10033.

(7) Lee, S.; Yuen, K. K.; Jolliffe, K. A.; Yoon, J. Fluorescent and colorimetric chemosensors for pyrophosphate. *Chem. Soc. Rev.* **2015**, *44* (7), 1749−1762.

(8) Satija, J.; Punjabi, N.; Mishra, D.; Mukherji, S. Plasmonic-ELISA: expanding horizons. *RSC Adv.* **2016**, *6* (88), 85440−85456.

(9) Peng, M.-P.; Ma, W.; Long, Y.-T. Alcohol dehydrogenase-catalyzed gold nanoparticle seed-mediated growth allows reliable detection of disease biomarkers with the naked eye. *Anal. Chem.* **2015**, *87* (12), 5891−5896.

(10) Ghosh, S. K.; Pal, T. Interparticle coupling effect on the surface plasmon resonance of gold nanoparticles: From theory to applications. *Chem. Rev.* **2007**, *107* (11), 4797−4862.

(11) Willets, K. A.; van Duyne, R. P. Localized surface plasmon resonance spectroscopy and sensing. *Annu. Rev. Phys. Chem.* **2007**, *58* (1), 267−297.

(12) Jeong, H. H.; Mark, A. G.; Alarcon-Correa, M.; Kim, I.; Oswald, P.; Lee, T. C.; Fischer, P. Dispersion and shape engineered plasmonic nanosensors. *Nat. Commun.* **2016**, *7*, 11331−11337.

(13) Li, M.; Shi, L.; Xie, T.; Jing, C.; Xiu, G.; Long, Y. T. An ultrasensitive plasmonic nanosensor for aldehydes. *ACS Sens.* **2017**, *2* (2), 263−267.

(14) Liu, B.; Liu, J. Methods for preparing DNA-functionalized gold nanoparticles, a key reagent of bioanalytical chemistry. *Anal. Methods* **2017**, *9* (18), 2633−2643.

DOI: 10.1021/acssensors.9b00438
ACS Sens. 2019, 4, 782−791

(15) Masson, J. F. Surface plasmon resonance clinical biosensors for medical diagnostics. *ACS Sens.* **2017**, *2* (1), 16−30.
(16) Yu, R.-J.; Ma, W.; Liu, X.-Y.; Jin, H.-Y.; Han, H.-X.; Wang, H.-Y.; Tian, H.; Long, Y.-T. Metal-linked immunosorbent assay (MeLISA): the enzyme-free alternative to ELISA for biomarker detection in serum. *Theranostics* **2016**, *6* (10), 1732−1739.
(17) Unser, S.; Bruzas, I.; He, J.; Sagle, L. Localized Surface Plasmon Resonance Biosensing: Current Challenges and Approaches. *Sensors* **2015**, *15* (7), 15684−15716.
(18) Zhang, Z.; Zhang, X.; Liu, B.; Liu, J. Molecular Imprinting on Inorganic Nanozymes for Hundred-fold Enzyme Specificity. *J. Am. Chem. Soc.* **2017**, *139* (15), 5412−5419.
(19) Cai, R.; Yang, D.; Peng, S.; Chen, X.; Huang, Y.; Liu, Y.; Hou, W.; Yang, S.; Liu, Z.; Tan, W. Single Nanoparticle to 3D Supercage: Framing for an Artificial Enzyme System. *J. Am. Chem. Soc.* **2015**, *137* (43), 13957−13963.
(20) Borghei, Y.-S.; Hosseini, M.; Dadmehr, M.; Hosseinkhani, S.; Ganjali, M. R.; Sheikhnejad, R. Visual detection of cancer cells by colorimetric aptasensor based on aggregation of gold nanoparticles induced by DNA hybridization. *Anal. Chim. Acta* **2016**, *904*, 92−97.
(21) Zhang, Z.; Chen, Z.; Cheng, F.; Zhang, Y.; Chen, L. Highly sensitive on-site detection of glucose in human urine with naked eye based on enzymatic-like reaction mediated etching of gold nanorods. *Biosens. Bioelectron.* **2017**, *89*, 932−936.
(22) Zhang, Z.; Chen, Z.; Wang, S.; Cheng, F.; Chen, L. Iodine-mediated etching of gold nanorods for plasmonic ELISA based on colorimetric detection of alkaline phosphatase. *ACS Appl. Mater. Interfaces* **2015**, *7* (50), 27639−27645.
(23) Larguinho, M.; Canto, R.; Cordeiro, M.; Pedrosa, P.; Fortuna, A.; Vinhas, R.; Baptista, P. V. Gold nanoprobe-based non-crosslinking hybridization for molecular diagnostics. *Expert Rev. Mol. Diagn.* **2015**, *15* (10), 1355−1368.
(24) Howes, P. D.; Chandrawati, R.; Stevens, M. M. Colloidal nanoparticles as advanced biological sensors. *Science* **2014**, *346* (6205), 1247390−1247390.
(25) Nie, L.; Liu, F.; Ma, P.; Xiao, X. Applications of gold nanoparticles in optical biosensors. *J. Biomed. Nanotechnol.* **2014**, *10* (10), 2700−2721.
(26) Priyadarshini, E.; Pradhan, N. Gold nanoparticles as efficient sensors in colorimetric detection of toxic metal ions: A review. *Sens. Actuators, B* **2017**, *238*, 888−902.
(27) Qin, L.; Zeng, G.; Lai, C.; Huang, D.; Xu, P.; Zhang, C.; Cheng, M.; Liu, X.; Liu, S.; Li, B.; Yi, H. Gold rush" in modern science: Fabrication strategies and typical advanced applications of gold nanoparticles in sensing. *Coord. Chem. Rev.* **2018**, *359*, 1−31.
(28) Tang, L.; Li, J. Plasmon-based colorimetric nanosensors for ultrasensitive molecular diagnostics. *ACS Sens.* **2017**, *2* (7), 857−875.
(29) Zhou, W.; Gao, X.; Liu, D.; Chen, X. Gold Nanoparticles for In Vitro Diagnostics. *Chem. Rev.* **2015**, *115* (19), 10575−10636.
(30) Sabela, M.; Balme, S.; Bechelany, M.; Janot, J.-M.; Bisetty, K. A review of gold and silver nanoparticle-based colorimetric sensing assays. *Adv. Eng. Mater.* **2017**, *19* (12), 1700270−1700293.
(31) Xianyu, Y.; Chen, Y.; Jiang, X. Horseradish peroxidase-mediated, iodide-catalyzed cascade reaction for plasmonic immunoassays. *Anal. Chem.* **2015**, *87* (21), 10688−10692.
(32) Yun, W.; Jiang, J.; Cai, D.; Zhao, P.; Liao, J.; Sang, G. Ultrasensitive visual detection of DNA with tunable dynamic range by using unmodified gold nanoparticles and target catalyzed hairpin assembly amplification. *Biosens. Bioelectron.* **2016**, *77*, 421−427.
(33) Zhang, Z.; Wang, H.; Chen, Z.; Wang, X.; Choo, J.; Chen, L. Plasmonic colorimetric sensors based on etching and growth of noble metal nanoparticles: strategies and applications. *Biosens. Bioelectron.* **2018**, *114*, 52−65.
(34) Chen, H.; Shao, L.; Li, Q.; Wang, J. Gold nanorods and their plasmonic properties. *Chem. Soc. Rev.* **2013**, *42* (7), 2679−2724.
(35) Jing, C.; Shi, L.; Liu, X.; Long, Y.-T. A single gold nanorod as a plasmon resonance energy transfer based nanosensor for high-sensitivity Cu (II) detection. *Analyst* **2014**, *139* (24), 6435−6439.
(36) Xie, T.; Jing, C.; Ma, W.; Ding, Z.; Gross, A. J.; Long, Y.-T. Real-time monitoring for the morphological variations of single gold nanorods. *Nanoscale* **2015**, *7* (2), 511−517.
(37) Cao, J.; Sun, T.; Grattan, K. T. V. Gold nanorod-based localized surface plasmon resonance biosensors: A review. *Sens. Actuators, B* **2014**, *195*, 332−351.
(38) Ma, X.; Chen, Z.; Kannan, P.; Lin, Z.; Qiu, B.; Guo, L. Gold nanorods as colorful chromogenic substrates for semiquantitative detection of nucleic acids, proteins, and small molecules with the naked eye. *Anal. Chem.* **2016**, *88* (6), 3227−3234.
(39) Gan, S. D.; Patel, K. R. Enzyme immunoassay and enzyme-linked immunosorbent assay. *J. Invest. Dermatol.* **2013**, *133* (9), e12.
(40) Apilux, A.; Ukita, Y.; Chikae, M.; Chailapakul, O.; Takamura, Y. Development of automated paper-based devices for sequential multistep sandwich enzyme-linked immunosorbent assays using inkjet printing. *Lab Chip* **2013**, *13* (1), 126−135.
(41) Berg, B.; Cortazar, B.; Tseng, D.; Ozkan, H.; Feng, S.; Wei, Q.; Chan, R. Y.-L.; Burbano, J.; Farooqui, Q.; Lewinski, M. Cellphone-based hand-held microplate reader for point-of-care testing of enzyme-linked immunosorbent assays. *ACS Nano* **2015**, *9* (8), 7857−7866.
(42) Toh, S. Y.; Citartan, M.; Gopinath, S. C.; Tang, T.-H. Aptamers as a replacement for antibodies in enzyme-linked immunosorbent assay. *Biosens. Bioelectron.* **2015**, *64*, 392−403.
(43) Thiha, A.; Ibrahim, F. A colorimetric enzyme-linked immunosorbent assay (ELISA) detection platform for a point-of-care dengue detection system on a lab-on-compact-disc. *Sensors* **2015**, *15* (5), 11431−11441.
(44) Martell, J. D.; Yamagata, M.; Deerinck, T. J.; Phan, S.; Kwa, C. G.; Ellisman, M. H.; Sanes, J. R.; Ting, A. Y. A split horseradish peroxidase for the detection of intercellular protein−protein interactions and sensitive visualization of synapses. *Nat. Biotechnol.* **2016**, *34* (7), 774−785.
(45) Zhao, Y.; Zheng, Y.; Kong, R.; Xia, L.; Qu, F. Ultrasensitive electrochemical immunosensor based on horseradish peroxidase (HRP)-loaded silica-poly (acrylic acid) brushes for protein biomarker detection. *Biosens. Bioelectron.* **2016**, *75*, 383−388.
(46) Busa, L. S. A.; Komatsu, T.; Mohammadi, S.; Maeki, M.; Ishida, A.; Tani, H.; Tokeshi, M. 3, 3′, 5, 5′-Tetramethylbenzidine oxidation on paper devices for horseradish peroxidase-based assays. *Anal. Sci.* **2016**, *32* (8), 815−818.
(47) Chen, C.; Zhao, D.; Sun, J.; Yang, X. Colorimetric logic gate for pyrophosphate and pyrophosphatase via regulating the catalytic capability of horseradish peroxidase. *ACS Appl. Mater. Interfaces* **2016**, *8* (43), 29529−29535.
(48) Bonifert, G.; Folkes, L.; Gmeiner, C.; Dachs, G.; Spadiut, O. Recombinant horseradish peroxidase variants for targeted cancer treatment. *Cancer Med.* **2016**, *5* (6), 1194−1203.
(49) Chen, P.; Liu, X.; Goyal, G.; Tran, N. T.; Shing Ho, J. C.; Wang, Y.; Aili, D.; Liedberg, B. Nanoplasmonic sensing from the human vision perspective. *Anal. Chem.* **2018**, *90* (7), 4916−4924.
(50) Ran, B.; Xianyu, Y.; Dong, M.; Chen, Y.; Qian, Z.; Jiang, X. Bioorthogonal reaction-mediated elisa using peroxide test strip as signal readout for point-of-care testing. *Anal. Chem.* **2017**, *89* (11), 6113−6119.
(51) Bos, E.; Van der Doelen, A.; Rooy, N. v.; Schuurs, A. H. 3, 3′, 5, 5′-Tetramethylbenzidine as an Ames test negative chromogen for horse-radish peroxidase in enzyme-immunoassay. *J. Immunoassay* **1981**, *2* (3−4), 187−204.
(52) Frey, A.; Meckelein, B.; Externest, D.; Schmidt, M. A. A stable and highly sensitive 3, 3′, 5, 5′-tetramethylbenzidine-based substrate reagent for enzyme-linked immunosorbent assays. *J. Immunol. Methods* **2000**, *233* (1−2), 47−56.
(53) Ma, X.; Lin, Y.; Guo, L.; Qiu, B.; Chen, G.; Yang, H.-h.; Lin, Z. A universal multicolor immunosensor for semiquantitative visual detection of biomarkers with the naked eyes. *Biosens. Bioelectron.* **2017**, *87*, 122−128.
(54) Lin, Y.; Zhao, M.; Guo, Y.; Ma, X.; Luo, F.; Guo, L.; Qiu, B.; Chen, G.; Lin, Z. Multicolor colormetric biosensor for the

DOI: 10.1021/acssensors.9b00438
ACS Sens. 2019, 4, 782−791

determination of glucose based on the etching of gold nanorods. *Sci. Rep.* **2016**, *6*, 37879−37885.
(55) Chen, Z.; Chen, C.; Huang, H.; Luo, F.; Guo, L.; Zhang, L.; Lin, Z.; Chen, G. Target-induced horseradish peroxidase deactivation for multicolor colorimetric assay of hydrogen sulfide in rat brain microdialysis. *Anal. Chem.* **2018**, *90* (10), 6222−6228.
(56) Ni, W.; Kou, X.; Yang, Z.; Wang, J. Tailoring longitudinal surface plasmon wavelengths, scattering and absorption cross sections of gold nanorods. *ACS Nano* **2008**, *2* (4), 677−686.
(57) Brillas, E.; Sirés, I.; Oturan, M. A. Electro-Fenton process and related electrochemical technologies based on Fenton's reaction chemistry. *Chem. Rev.* **2009**, *109* (12), 6570−6631.
(58) El Harrad, L.; Amine, A. Amperometric biosensor based on prussian blue and nafion modified screen-printed electrode for screening of potential xanthine oxidase inhibitors from medicinal plants. *Enzyme Microb. Technol.* **2016**, *85*, 57−63.
(59) Dervisevic, M.; Custiuc, E.; Çevik, E.; Şenel, M. Construction of novel xanthine biosensor by using polymeric mediator/MWCNT nanocomposite layer for fish freshness detection. *Food Chem.* **2015**, *181*, 277−283.
(60) Cela-Pérez, M.; Barbosa-Pereira, L.; Vecino, X.; Pérez-Ameneiro, M.; Latorre, A. L.; López-Vilariño, J.; Rodríguez, M. G.; Moldes, A.; Cruz, J. Selective removal of ATP degradation products from food matrices II: Rapid screening of hypoxanthine and inosine by molecularly imprinted matrix solid-phase dispersion for evaluation of fish freshness. *Talanta* **2015**, *135*, 58−66.
(61) Hong, H.; Regenstein, J. M.; Luo, Y. The importance of ATP-related compounds for the freshness and flavor of post-mortem fish and shellfish muscle: A review. *Crit. Rev. Food Sci. Nutr.* **2015**, *57* (9), 1787−1798.
(62) Chen, Z.; Lin, Y.; Ma, X.; Guo, L.; Qiu, B.; Chen, G.; Lin, Z. Multicolor biosensor for fish freshness assessment with the naked eye. *Sens. Actuators, B* **2017**, *252*, 201−208.
(63) Lin, Y.; Xu, S.; Yang, J.; Huang, Y.; Chen, Z.; Qiu, B.; Lin, Z.; Chen, G.; Guo, L. Interesting optical variations of the etching of Au Nanobipyramid@ Ag Nanorods and its application as a colorful chromogenic substrate for immunoassays. *Sens. Actuators, B* **2018**, *267*, 502−509.
(64) Xia, Y.; Ye, J.; Tan, K.; Wang, J.; Yang, G. Colorimetric visualization of glucose at the submicromole level in serum by a homogenous silver nanoprism−glucose oxidase system. *Anal. Chem.* **2013**, *85* (13), 6241−6247.
(65) Yang, X.; Yu, Y.; Gao, Z. A Highly Sensitive Plasmonic DNA Assay Based on Triangular Silver Nanoprism Etching. *ACS Nano* **2014**, *8* (5), 4902−4907.
(66) Rivero, P. J.; Goicoechea, J.; Urrutia, A.; Arregui, F. J. Effect of both protective and reducing agents in the synthesis of multicolor silver nanoparticles. *Nanoscale Res. Lett.* **2013**, *8* (1), 101−109.
(67) Yen, C.-W.; de Puig, H.; Tam, J. O.; Gómez-Márquez, J.; Bosch, I.; Hamad-Schifferli, K.; Gehrke, L. Multicolored silver nanoparticles for multiplexed disease diagnostics: distinguishing dengue, yellow fever, and Ebola viruses. *Lab Chip* **2015**, *15* (7), 1638−1641.
(68) Millán, J. L.; Whyte, M. P. Alkaline phosphatase and hypophosphatasia. *Calcif. Tissue Int.* **2016**, *98* (4), 398−416.
(69) Li, G.; Fu, H.; Chen, X.; Gong, P.; Chen, G.; Xia, L.; Wang, H.; You, J.; Wu, Y. Facile and sensitive fluorescence sensing of alkaline phosphatase activity with photoluminescent carbon dots based on inner filter effect. *Anal. Chem.* **2016**, *88* (5), 2720−2726.
(70) Gao, Z.; Deng, K.; Wang, X.-D.; Miró, M.; Tang, D. High-resolution colorimetric assay for rapid visual readout of phosphatase activity based on gold/silver core/shell nanorod. *ACS Appl. Mater. Interfaces* **2014**, *6* (20), 18243−18250.
(71) Chen, J.; Jackson, A. A.; Rotello, V. M.; Nugen, S. R. Colorimetric detection of escherichia coli based on the enzyme-induced metallization of gold nanorods. *Small* **2016**, *12* (18), 2469−2475.
(72) Yang, X.; Gao, Z. Enzyme-catalysed deposition of ultrathin silver shells on gold nanorods: a universal and highly efficient signal amplification strategy for translating immunoassay into a litmus-type test. *Chem. Commun.* **2015**, *51* (32), 6928−6931.
(73) Li, Y.; Ma, X.; Xu, Z.; Liu, M.; Lin, Z.; Qiu, B.; Guo, L.; Chen, G. Multicolor ELISA based on alkaline phosphatase-triggered growth of Au nanorods. *Analyst* **2016**, *141* (10), 2970−2976.
(74) Xu, S.; Ouyang, W.; Xie, P.; Lin, Y.; Qiu, B.; Lin, Z.; Chen, G.; Guo, L. Highly uniform gold nanobipyramids for ultrasensitive colorimetric detection of influenza virus. *Anal. Chem.* **2017**, *89* (3), 1617−1623.
(75) Park, G.; Lee, C.; Seo, D.; Song, H. Full-Color Tuning of Surface Plasmon Resonance by Compositional Variation of Au@Ag Core−Shell Nanocubes with Sulfides. *Langmuir* **2012**, *28* (24), 9003−9009.
(76) Wang, Y.; Zhang, P.; Mao, X.; Fu, W.; Liu, C. Seed-mediated growth of bimetallic nanoparticles as an effective strategy for sensitive detection of vitamin C. *Sens. Actuators, B* **2016**, *231*, 95−101.
(77) Guo, Y.; Wu, J.; Li, J.; Ju, H. A plasmonic colorimetric strategy for biosensing through enzyme guided growth of silver nanoparticles on gold nanostars. *Biosens. Bioelectron.* **2016**, *78*, 267−273.
(78) Alex, S. A.; Chandrasekaran, N.; Mukherjee, A. State-of-the-art strategies for the colorimetric detection of heavy metals using gold nanorods based on aspect ratio reduction. *Anal. Methods* **2016**, *8* (10), 2131−2137.
(79) Liu, Y.; Lv, B.; Liu, A.; Liang, G.; Yin, L.; Pu, Y.; Wei, W.; Gou, S.; Liu, S. Multicolor sensor for organophosphorus pesticides determination based on the bi-enzyme catalytic etching of gold nanorods. *Sens. Actuators, B* **2018**, *265*, 675−681.

DOI: 10.1021/acssensors.9b00438
ACS Sens. 2019, 4, 782−791